LANGMUIR Article
Cite This: Langmuir XXXX, XXX, XXX−XXX
pubs.acs.org/Langmuir

Interface Bonding Properties and Mechanism of Poplar Board-Veneered Wood Fiber/Polypropylene Composites with Chlorinated Polypropylene Films as an Intermediate Layer

Yinan Liu,[†,‡] Yanan Sun,[†] Jianxiu Hao,[†] Weihong Wang,[*,†] Yongming Song,[†] and Zhifang Zhou[‡]

[†]Key Laboratory of Bio-Based Material Science and Technology (Chinese Ministry of Education), Northeast Forestry University, Harbin 150040, China

[‡]Heilongjiang Institute of Wood Science, Harbin 150040, China

ABSTRACT: It is difficult to decorate wood plastic composites with wood veneer because their surface energy is low and there are no pores on the surface. In the present study, we developed an environmentally friendly and convenient method to decorate the wood fiber/polypropylene (WF/PP) composite board. We used chlorinated polypropylene (CPP) as an intermediate film to laminate wood veneer to WF/PP composite boards by hot-pressing at 110 °C and then cooling down. The interface bonding mechanism between the wood veneer, CPP layer, and WF/PP composite was analyzed using scanning electron microscopy (SEM), energy dispersive X-ray analysis (EDS), surface roughness test, and attenuated total reflection−Fourier transform infrared spectroscopy (ATR−FTIR). The results indicated that CPP penetrated the wood pores and formed a firm anchor structure. SEM images showed small cracks at the interface between CPP and PP when WF/PP contained less WF. The results of SEM−EDS and ATR−FTIR showed that WF/PP composites with a higher WF content would have more fibers exposed at the surface, thus making the surface rough and providing more specific surface area. The veneered WF/PP composite with 80% WF content had the highest surface bond strength and water resistance.

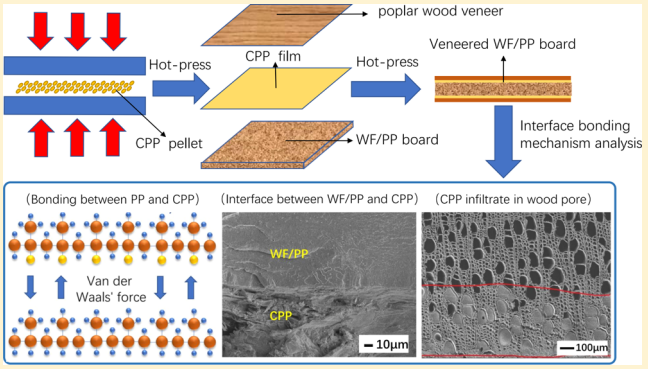

1. INTRODUCTION

The connection between the dwelling environment and human health has been a focus of governments worldwide in recent years.[1−3] Commonly used materials for indoor decoration (e.g., shaving board, fiberboard, and aldehyde adhesive) contain volatile organic matter.[4,5] Many research institutions have attempted to find a substitute material for traditional wood-based boards. The biofiber-reinforced polyolefin composite is a suitable material that does not contain volatile matter. The processing residue of wood products and nondegradable high-density polyethylene polypropylene (PP) can be recycled as a raw material. Biofiber-reinforced polyolefin composites have good mechanical properties[6] and possess dimensional stability and water resistance. Furthermore, the addition of biofiber could improve impact strength and elasticity. However, the nonporosity and nonpolar surface characteristics of polyolefin-based composites result in difficult coverage with common adhesives compared to the traditional artificial wood boards. This limits the application of the polyolefin matrix composite in the interior environment region.

PP is a commonly used matrix material for manufacturing biofiber-reinforced polyolefin composites.[7] Several studies have investigated the enhancement and interfacial modification of biofiber-reinforced PP composites over recent years.[8,9] Beg (2016) used NaOH to pretreat wood fiber (WF) and obtained the enhancement effect of materials.[9] On the basis of alkali treatment, Ma (2017) treated hemp with 3-aminopropyltriethoxysilane and achieved an even better result.[10] As well as chemical treatment, the addition of compatibilizers is also an effective method. Karmarkar (2007) grafted *m*-isopropenyl-α, α-dimethylbenzyl-isocyanate onto PP to enhance the interface bond between the WF and PP matrix.[11] Both the tensile strength and flex properties of the resultant composite were significantly improved. These treatments may be efficient in modifying the surface of biofiber-reinforced PP composites, but they require high temperatures or a cumbersome process to react. As a physical method, plasma treatment of the surface of polyolefin materials was investigated,[12,13] which temporarily increased the ion activity on the material surface. Gupta (2007) and Laborie (2007) used flame and plasma to treat the surface of biofiber-reinforced PP by increasing oxygen-containing groups.[14,15] However, these treatments have limitations, including the effect not being maintained for a long period of time. Chemical modification on the surface maybe a better way to enhance the adhesion properties,[16,17] but the high cost and pollution produced during treatment

Received: July 19, 2019
Revised: September 22, 2019
Published: October 1, 2019

DOI: 10.1021/acs.langmuir.9b02241
Langmuir XXXX, XXX, XXX−XXX

impeded its application for industries. Guo et al. (2018) used the MAPE and HDPE film as an intermediate layer,[18] which solved the problems of pollution and bonding strength, but the high temperature required would melt the base biofiber-reinforced board as well as degrade the surface decorating materials.

In this study we explored a new technology for decorating the WF/PP composite board by using an intermediate film as an adhesive at a lower hot-pressing temperature. Chlorinated polypropylene (CPP) was used to bond the wood veneer and WF/PP composite base board. CPP is often used as a modifying agent in coatings and adhesives. Hu et al. (2018) synthesized a CPP emulsion by grafting methyl methacrylate,[19] butyl acrylate, and acrylic acid onto it. The printability of the PP film was improved after coating with the modified CPP emulsion. Tomasetti et al. (2000) found that CPP solution could diffuse into the PP/PE copolymer.[20] On the other hand, the grafting of chlorine (Cl) in the molecular chain increased the polarity of CPP, thus improving its adhesion to the wooden surface. CPP could, therefore, be used as an advanced intermediate adhesive for the lamination of the PP board with other materials.

The lamination process was conducted at a relatively low temperature (90−110 °C), therefore avoiding the deformation of the WF/PP base board (PP melting point was 168 °C in this study) and degradation of the wood veneer surface. The bonding strength and water resistance of the adhesive layer were investigated. The bonding mechanism between the wood veneer, CPP, and WF/PP was built based on analyzing the penetration of CPP into wood conduits, surface roughness, and chemical characteristics of the composite surface. A simulation experiment of CPP and PP bonding was implemented to reveal the real form of their interface. The proposed method is simple and environmentally friendly.

2. EXPERIMENTAL SECTION

2.1. Materials. The rotary-cut Poplar wood (*Populus tomentosa* Carrière) veneers (thickness of 1.5 ± 0.1 mm) were purchased from Jinan Yuanfang Wood Trading Company. The moisture content of these veneers was 28%. Some of the veneers were ground (40−80 mesh) to WFs for preparing the WF/PP composite. WFs and veneers were dried at a temperature of 103 °C until the moisture content was <3.0%. PP (T300, melting point 168 °C, density 0.91 g/cm^3, melting flow rate (MFR) = 2.5−3.5 g/10 min at 180 °C) was purchased from Sinopec Daqing Petrochemical Company, Daqing, China. Maleic anhydride grafted polypropylene (MAPP) (grafting percentage 1−1.2%) was obtained from Shanghai Sunny New Technology Development Co, Shanghai, China. CPP was supplied as pellets by Shenzhen Jitian Chemical Products Limited Company, Shenzhen, China, with a chlorination ratio of 32%, MFR = 16.6−20.1 g/10 min at 110 °C, melting point 90 °C, and density 0.93 g/cm^3.

2.2. Preparation of WF/PP Composites. PP, WF, and MAPP were blended at different mass fraction ratios (Table 1) with a high-speed mixer (SHR-10A, Zhangjiagang Tonghe Plastic Machinery Co, Zhangjiagang, China). The mixtures were prilled using a corotating twin-screw extruder (JSH30, Nanjing Rubber & Plastic Machinery, Nanjing, China) and cut into small granules with a pulverizer. These particles were extruded into WF/PP composite boards (4 mm thick, 100 mm wide) through a single-screw extruder (SJ45, Nanjing Rubber and Plastics Machinery Factory, China). Three ratios of WF to PP were synthesized, as shown in Table 1.

Table 1. Component Mass Parts for Each WF/PP Composite (Mass Part)

composite	WF	PP	MAPP
60 WF/40 PP	60	40	2
70 WF/30 PP	70	30	1.5
80 WF/20 PP	80	20	1

2.3. Preparation of CPP Films. The CPP film preparation process is shown in Figure 1. The CPP particles were evenly spread in a square mold with an inside length of 160 mm and a thickness of 0.1 mm. The mold was hot-pressed at a temperature of 110 °C for 3 min, under a pressure of 2 MPa. It was then cold-pressed at a temperature of 20 °C for 5 min to shape the film.

2.4. Preparation of the Veneered WF/PP Composite Board. The surface of the WF/PP composite board was covered with the CPP film, onto which the poplar veneer was then placed, as shown in Figure 1. The sandwich structure was pressed under a pressure of 5 MPa for 5 min at a temperature of 110 °C and then cold-pressed at a temperature of 20 °C for 5 min.

As a control, the WF/PP composite board containing 60% WF was covered with wood veneer by pressing at 180 °C without an intermediate film or adhesive. PP accumulated on the surface of the WF/PP composite acting as a "glue".

The veneered WF/PP boards were then conditioned at a temperature of 20 °C and 65% relative humidity for 1 week before they were tested.

2.5. Preparation of CPP/PP Compound Films. In order to detect the bonding mechanism between the CPP and PP accumulated on the surface of the WF/PP composite, a CPP/PP compound film was prepared. CPP and PP particles were hot-pressed into films at a temperature of 110 and 180 °C, respectively, and then cold-pressed at a temperature of 20 °C. The two films were then laminated together at a temperature of 110 °C (same as the preparation of the veneered WF/PP composite board, in Section 2.4). The CPP/PP compound film had two surfaces, that is, one side was CPP and the other was PP. The process for preparing and analyzing the CPP/PP compound film is shown in Figure 2. The three surfaces of the compound film were scanned with scanning electron microscopy (SEM) is shown in Figure 2.

2.6. Measuring the Penetration Depth of CPP and PP into the Wood Veneer. To illustrate the bonding mechanism between PP, CPP, and the wood veneer, we designed an experiment to simulate the bonding between CPP, PP, and the wood board. The CPP film was prepared and spread on the poplar wood veneer, then pressed together at 110 °C and 2 MPa for 2 min. The board was cooled to room temperature and cut into slices with a microtome. The PP film-covered veneer was prepared in the same way but pressed at a temperature of 180 °C. The cross-section of microsections was scanned with scanning electron microscopy (SEM).

2.7. Surface Bonding Strength Test. The surface bonding strength between the veneer and WF/PP board was evaluated based on the vertical drawing test as shown in Figure 3. The size of the sample was 50 × 50 × 6 mm^3, with a middle circle of 1000 mm^2 area curved on the surface. There were 12 specimens in each group. The loading rate was 2 mm/s.

2.8. Water Resistance Test. The water resistance of the adhesive layer and its interfaces between the wood veneer and WF/PP composite board was evaluated. Samples (veneered WF/PP composites, 75 × 75 × 6 mm^3) were immersed in water at 63 °C for 3 h and then dried in an oven at 63 °C for 3 h. The delaminated length at four edges of the dried samples was measured. Six samples were tested in each series.

2.9. Surface Roughness Test. The surface roughness of the WF/PP base board was measured using a contact-type surface roughness measuring instrument (SJ-210, Mitutoyo Japan Corporation, Kawasaki, Japan). The maximum height of the profile (R_z), contour arithmetic means deviation (R_a), surface profile height root mean square (R_q), and the surface contour curve were measured and calculated according to "ISO 4287:1997 geometrical product specifications, surface texture: profile method, terms, definitions, and surface texture parameters." The testing length was 5 mm. The

DOI: 10.1021/acs.langmuir.9b02241
Langmuir XXXX, XXX, XXX−XXX

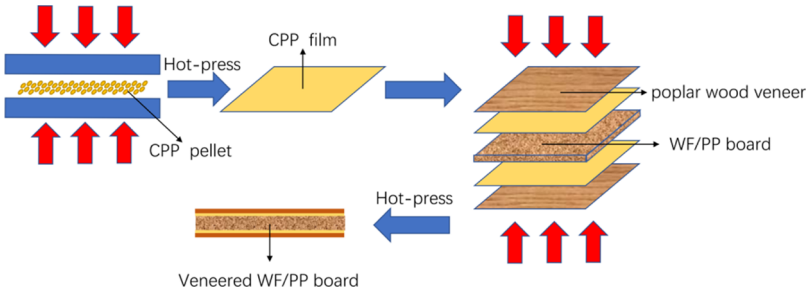

Figure 1. Process for the preparation of a veneered WF/PP board with CPP intermediate films.

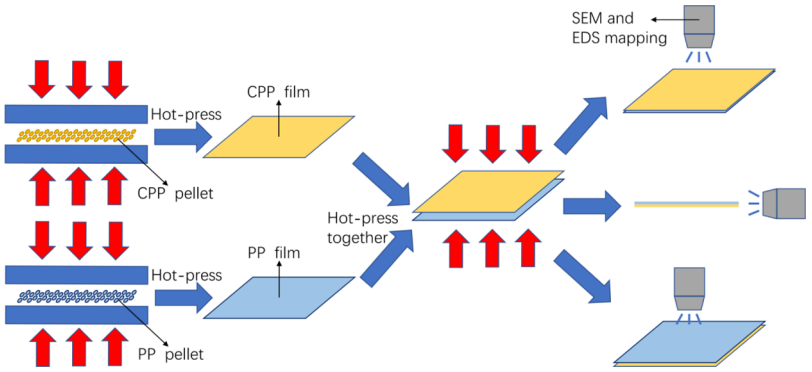

Figure 2. Process for lamination of CPP and PP and analysis of the bonding mechanism.

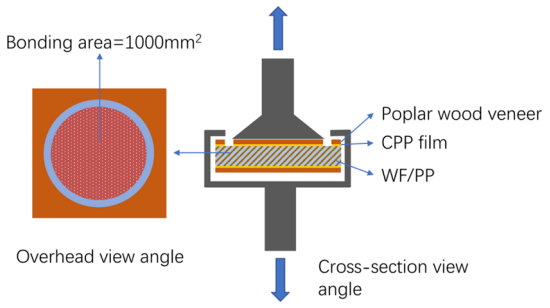

Figure 3. Schematic diagram showing the sample and apparatus used to test the surface bonding strength.

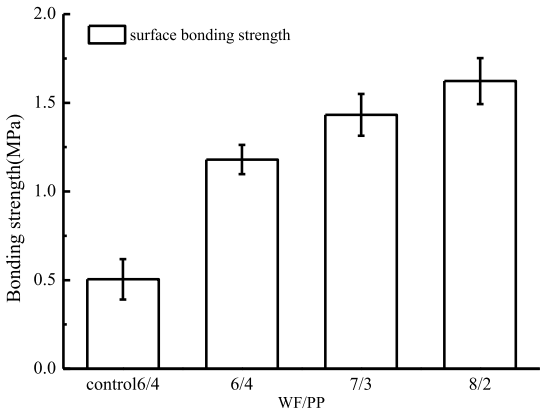

Figure 4. Surface bonding strength of wood veneered WF/PP composites.

probe was made of adamas, with a movement speed of 0.5 mm/s and a pressure of 4 mN. A GAUSS filter was used and 8000 data points were collected.

2.10. Scanning Electron Microscopy. The bonding interface between the WF/PP composite board and the poplar veneer was first observed under a scanning electron microscope (JSM7500F, JEOL DATUM Shanghai Co., Ltd. Shanghai, China). The section slices were prepared by microtomy (described above). The samples were coated with gold and then examined with an accelerating voltage of 5 kV. Two sides and the cross-section of the CPP/PP compound film were scanned by SEM and energy dispersive X-ray analysis (EDS) to confirm the Cl distribution. WF/PP boards were scanned in the same way to detect oxygen.

2.11. ATR–FTIR Spectroscopy. The chemical group on the surface of the WF/PP composite was analyzed with attenuated total reflection–Fourier transform infrared spectroscopy (ATR–FTIR) spectroscopy (Nicolet 6700, Nicolet Company, Madison, Wisconsin, USA). Scans were recorded from 4000 to 400 cm^{-1} at a resolution of 4 cm^{-1}. Six spectra curves were recorded for each sample.

3. RESULTS AND DISCUSSION

In this study, CPP was the key intermediate layer between the wood veneer and WF/PP composite board. The layer was in contact, on the one side, with the polar wood surface and the surface of the WF/PP composite on the other side. These two interfaces had very different combination modes and bonding strengths, which determined the bonding strength between the WF/PP base board and the wood veneer surface.

3.1. Bonding Strength of the Veneered WF/PP Composite. As shown in Figure 4, the bonding strength significantly increased with an increasing WF content of the WF/PP composite. The control group showed the lowest bonding strength and the layers separated between the wood veneer and base board (Figure 5a). The WF content in the WF/PP composite was the main factor influencing the bond strength for the sample with the CPP film. The failure region with fewer wood fragments stick on it (Figure 5b) for the base board with 60 mass part WF content. than that samples with higher WF content. With the increasing of the WF content in the base board, the surface failure position moved further inside the wood veneer (Figure 5c,d). No failure occurred on

DOI: 10.1021/acs.langmuir.9b02241
Langmuir XXXX, XXX, XXX–XXX

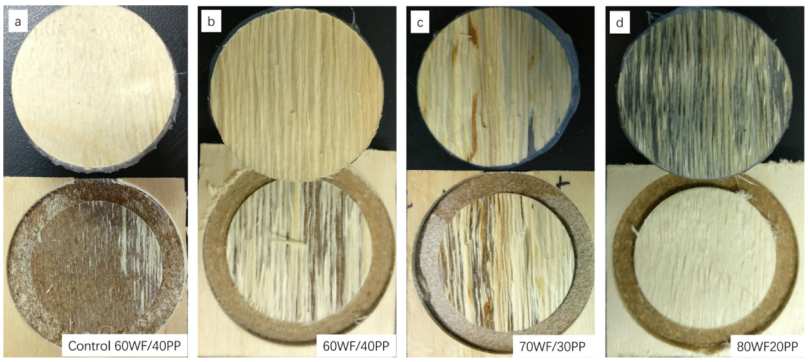

Figure 5. Failure morphology of the adhesive layer in (a) control; (b) 60 WF/40 PP base board; (c) 70 WF/30 PP base board; and (d) 80 WF/20 PP base board.

Table 2. Length of Delamination between Veneer and WF/PP Composites after Water Soaking–Drying Treatment

	WF/PP base board			
	control 60 WF/40 PP	60 WF/40 PP	70 WF/30 PP	80 WF/20 PP
delamination length (mm)	48.7	5.5	0.4	0

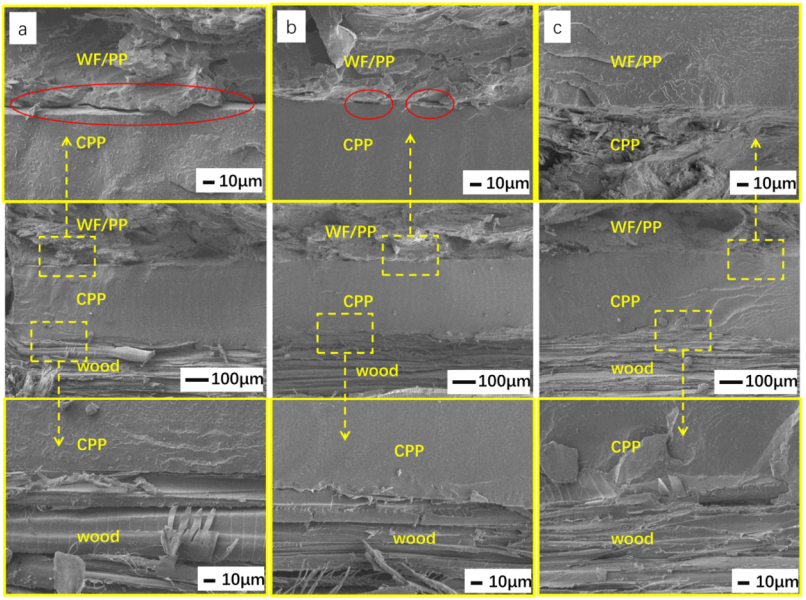

Figure 6. Cross-section of the interface between the wood veneer, CPP, and WF/PP for (a) 60 WF/40 PP; (b) 70 WF/30 PP; and (c) 80 WF/20 PP base board composites.

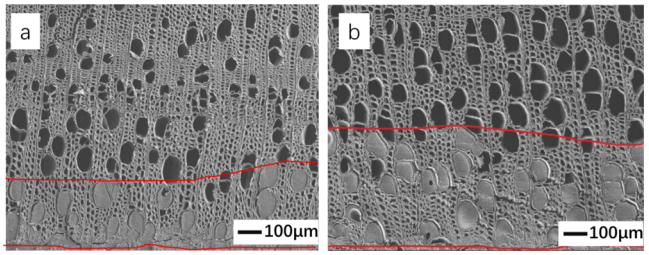

Figure 7. Penetration depth of CPP and PP into the poplar wood veneer. (a) PP penetration depth; and (b) CPP penetration depth.

the bond line of the sample with 80 mass part WF content, that is, all the failure occurred within the poplar wood veneer (Figure 5d). These results indicated that CPP provided a greater bonding strength to the veneered WF/PP composite with a higher WF content.

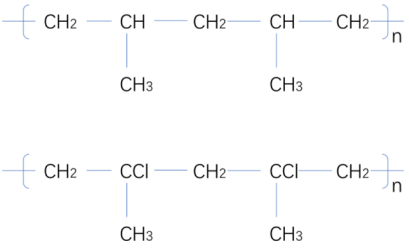

Figure 8. The molecular structures of PP (top) and CPP (bottom).

3.2. Water Resistance of the Glue Line. The delamination length of the four veneered WF/PP composites is shown in Table 2. The control group presented with the longest delamination. This was because hot water immersion and drying treatment caused expansion and shrinking of the wood veneer and rough surface of the WF/PP base board. The

DOI: 10.1021/acs.langmuir.9b02241
Langmuir XXXX, XXX, XXX–XXX

Table 3. Ratio of Cl in the CPP/PP Compound Film (%)

	element					
	CPP side		PP side		CPP/PP cross-section	
	C	Cl	C	Cl	C	Cl
atomic mass	75.37	24.63	99.8	0.2	92.83	7.17
atomic number	89.91	10.09	99.93	0.07	97.43	2.57

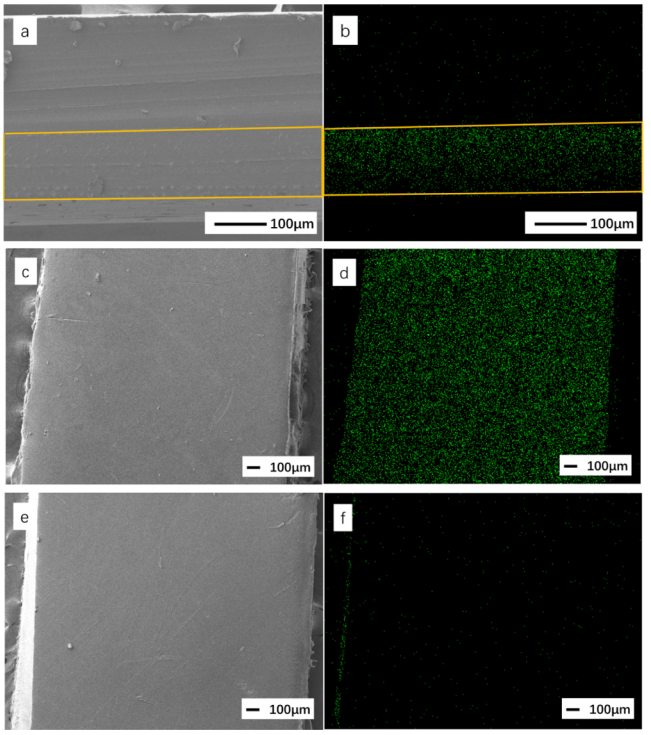

Figure 9. Distribution of Cl in the CPP/PP compound film. (a,b) Cross-section of the compound film; (c,d) CPP surface; and (e,f) PP surface.

60 WF/40 PP veneered composite sample had a delamination length of 5.5 mm, and the delamination lengths of the 70 WF/30 PP and 80 WF/20 PP composites were 0.4 and 0 mm, respectively. Thus, the delamination length shortened with an increasing WF content in the WF/PP material. The results indicated that the bond between the WF/PP composite-CPP-poplar wood board would withstand water intrusion and the strain of wood deformation. The bond strength was analyzed using SEM−EDS and ATR−FTIR.

3.3. Poplar Wood and CPP Interface. Figure 6 shows the glue line of the CPP film in the veneered WF/PP composites. There was no crevice between the CPP layer and the wood veneer, which indicated a firm bond. The CPP melted at 110 °C and penetrated into the wood conduits under pressure. After the cooling press, the CPP hardened and adhered to the wooden conduit wall. The glue line of the control laminate composite (laminate veneer and WF/PP without a CPP film) could not be observed because it could not withstand the impact force from sample preparation and separated at the bond line. Without the CPP intermediate layer, the bond strength between the veneer and WF/PP board was weak.

Figure 7 shows section views of the slices prepared (Section 2.5). The depth of penetration of CPP into the poplar wood veneer was 0.5−0.6 mm (Figure 7b). This deep penetration

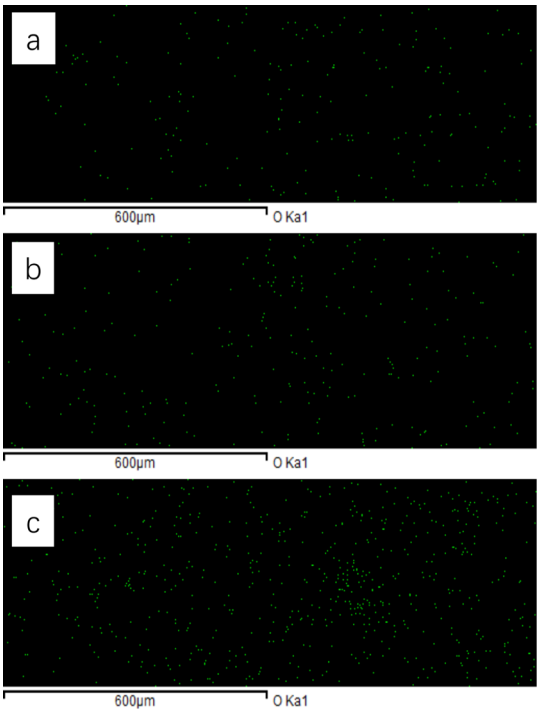

Figure 10. Distribution of oxygen on the WF/PP surface for the (a) 60 WF/40 PP; (b) 70 WF/30 PP; and (c) 80 WF/20 PP composites.

Table 4. Ratio of Oxygen on the WF/PP Surfaces

WF/PP composite	element					
	60 WF/40 PP		70 WF/30 PP		80 WF/20 PP	
	C	O	C	O	C	O
atomic mass	93.72	6.28	91.25	8.75	85.23	14.77
atomic number	95.21	4.79	93.29	6.71	88.49	11.51

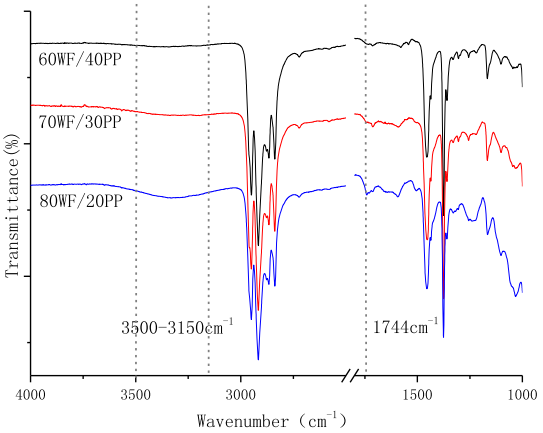

Figure 11. Surface chemical groups of the WF/PP base board.

provided a stable anchoring structure between CPP and the wood board. For the wood veneer/PP lamination without the intermediate CPP layer (Figure 7a), the PP penetrated only 0.3−0.4 mm into the wood veneer, that is, shallower than CPP. This created an obvious crevice between PP and the pore wall because nonpolar PP could not adhere to the polar surface of the wood.

CPP is more polar than pure PP because of the Cl grafting on the molecular chains. This allows it to bond more closely with the wood conduit wall. CPP also has a higher MFR than

DOI: 10.1021/acs.langmuir.9b02241
Langmuir XXXX, XXX, XXX−XXX

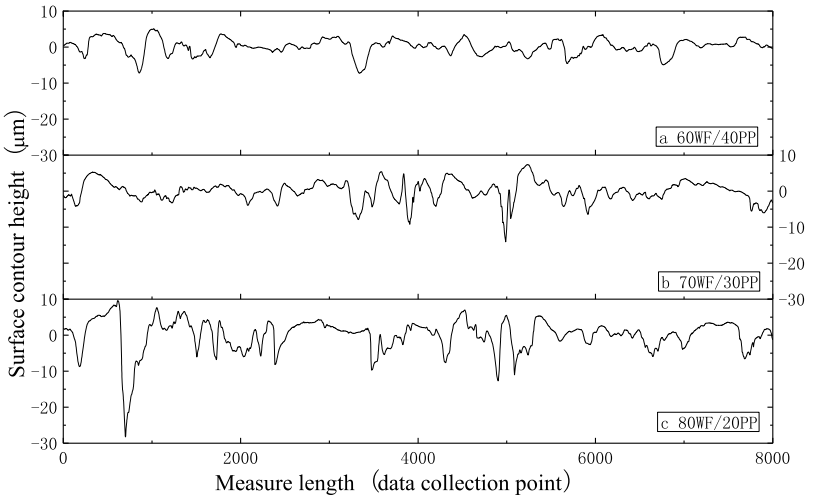

Figure 12. Surface contours of WF/PP composites. (a) 60 WF/40 PP; (b) 70 WF/30 PP; and (c) 80 WF/20 PP.

Table 5. Surface Roughness of the WF/PP Base Board Composites

WF/PP composite	R_a (μm)	R_z (μm)	R_q (μm)
60 WF/40 PP	1.583	9.069	2.048
70 WF/30 PP	2.080	12.501	2.680
80 WF/20 PP	3.206	19.090	4.098

PP and therefore could penetrate deeper into the porous wood. These factors greatly improved the bonding strength between the wood veneer and WF/PP composite base board.

3.4. WF/PP and CPP Interface. The bonding condition between the CPP and WF/PP composite was a very important factor to the surface bonding strength of the veneered composite. The WF/PP composite surface assembled a PP layer during the extrusion molding process. This PP layer would combine with the molten CPP during the hot-press. Because CPP has a similar molecular structure to PP (Figure 8), it is potentially easy for CPP to adhere to the PP surface.

Wood veneer was laminated with the WF/PP composite at 110 °C, which was lower than the melting point of PP (168 °C). The PP molecular chains deformed and displaced in a very limited range rather than move freely. However, CPP melted at 110 °C and moved freely into the interspace of the PP molecule chains, thus forming an absorption structure. To illustrate this, the CPP film and PP film were laminated at a temperature of 110 °C. Both sides of the compound film were scanned, and the number and Cl atomic mass of the scanned surface are shown in Table 3. On the CPP side, the atomic mass and Cl content was much greater than on the PP side. Figure 9a,b shows a cross-section of the PP/CPP compound film in which Cl is distributed in a limited region. This indicated that the PP and CPP molecular chains were not remarkably diffused and mixed. Figure 9c,d shows the CPP surface of the compound film where high Cl content was detected. On the PP side of the compound film (Figure 9e,f), the Cl content was low, showing that the CPP molecular chains could not diffuse to this side.

As shown in Figure 6c, there was no crevice between the CPP layer and WF/PP composite for the sample that contained 80 mass part WF, however, small gaps were observed (Figure 6a,b) for the composite with 60 and 70 mass part WF. The WF content in the composite therefore influenced the interface bonding between CPP and WF/PP. The roughness and specific area of the WF/PP base board was affected by the exposed WFs. High WF content provided the base board with more exposed WFs, as explained below (Sections 3.5 and 3.6).

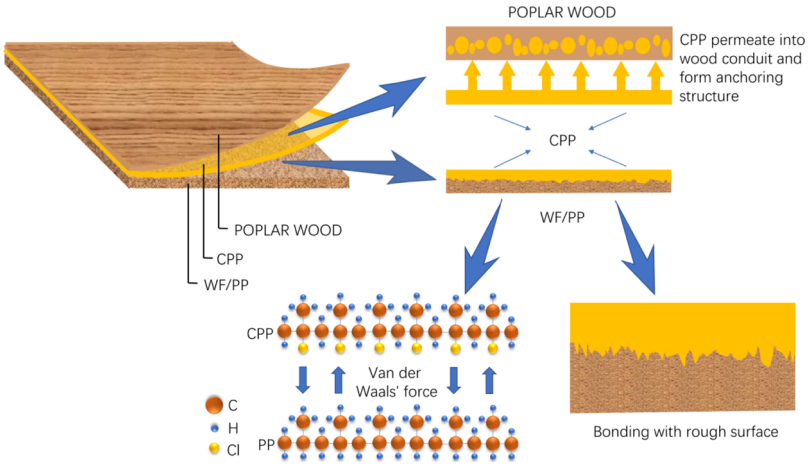

Figure 13. Interface bonding mechanism of the veneered WF/PP composite board.

DOI: 10.1021/acs.langmuir.9b02241
Langmuir XXXX, XXX, XXX−XXX

3.5. Elements on the WF/PP Composite Surface. Figure 10 shows the distribution of oxygen on the surface of the WF/PP composite. Oxygen is mainly contained in the hydroxy and carbonyl forms in WF. The carbonyl content of MAPP can be ignored as it is negligible. Therefore, we considered the content and distribution of oxygen as the exposed WF on the surface of the WF/PP composite. Compared to the 70 and 80 mass part WF composites, the 60 mass part WF composite (Figure 10a) showed the least oxygen distribution. Combining the atomic mass and atomic numbers listed in Table 4, it was obvious that the amount of oxygen increased with the increasing WF content in the WF/PP composite. This indicated that more WF would extrude out and increase the polarity of the surface after processing.

This phenomenon was in line with the results of the ATR−FTIR test shown in Figure 11. The strength of the "−OH" characteristic peak between 3150 and 3500 cm^{-1} represents the WF and intensified with the increasing WF content in the WF/PP composites. Meanwhile, the characteristic peak of the WF at 1744 cm^{-1} (stretching vibration of C═O of acetyl and carboxyl groups in hemicelluloses and carbonyl aldehyde in lignin and extractives) was also enhanced. These changes in peak strength indicated the WF content. On the other hand, increased fiber would increase the polarity of the base board surface, thus affecting its surface bonding affinity with other materials.

3.6. WF/PP Composite Surface Roughness. Surface roughness is an important factor affecting bond strength.[21,22] As shown in Figure 12, the surface contour height range increased with an increasing WF content in the WF/PP composite. Those rough surfaces could provide more specific surface area and embedded groove for molten CPP. Surface roughness parameters were calculated based on ISO 4287:1997 and are listed in Table 5. R_a and R_q represented the surface roughness, the higher value, respectively, which indicated greater roughness. R_z represented the maximum height from the lowest point to the highest. The R_a, R_q, and R_z parameters of WF/PP composites all increased with the increasing WF content. As stated above, this surface roughness was because of the exposed WFs, which did not form a smooth surface like PP. This roughness was a benefit for binding with CPP.

Based on the above investigation of the combined interfaces between the wood veneer, CPP layer, and WF/PP composite, the bonding model between polar wood veneer and nonpolar WF/PP board was proposed as shown in Figure 13. At a temperature of 110 °C CPP can melt and infiltrate into the porous wood veneer forming a firm anchoring structure. Though CPP and PP do not diffuse and mix at this temperature, they have similar molecular structures and form strong van der Waals forces between.

4. CONCLUSIONS

WF/PP is manufactured with recycled material and without the emission of volatile organic compounds. If its surface was more aesthetically pleasing, it could be used for interior decoration and furniture preparation. In this study we investigated CPP as an intermediate layer to bond poplar wood veneer to the WF/PP composite. The result was satisfactory.

All the veneered composite samples with a CPP bonding layer had good water resistance. The surface bonding strength could reach 1.2 MPa and much higher than the requirement of surface decoration. SEM−EDS and ATR−FTIR showed the amount of exposed WF on the surface of the WF/PP composite. The WF content of the WF/PP positively correlated with the surface bonding strength. The exposed WF on the WF/PP composite increased the surface roughness and polarity, promoting the formation of a strong surface bond. Thus, the bonding strength increased with an increasing WF content in the WF/PP base material.

AUTHOR INFORMATION

Corresponding Author

*E-mail: weihongwang2001@nefu.edu.

ORCID

Yinan Liu: 0000-0002-8785-4011

Notes

The authors declare no competing financial interest.

ACKNOWLEDGMENTS

This work was supported by the National Natural Science Foundation of China (31670573), Provincial Natural Science Foundation of Heilongjiang (ZD2016002), and the 2017 Special Project of Sustainable Development for Central University Innovation Team of the Ministry Educatio-n(2572017ET05). We thank International Science Editing (http://www. Internationalscienceediting.com) for editing this manuscript.

REFERENCES

(1) Salthammer, T.; Zhang, Y.; Mo, J.; Koch, H. M.; Weschler, C. J. Assessing Human Exposure to Organic Pollutants in the Indoor Environment. *Angew. Chem., Int. Ed. Engl.* **2018**, *57*, 12228−12263.

(2) Stewart, A.; Hursthouse, A. Environment and Human Health: The Challenge of Uncertainty in Risk Assessment. *Geosciences* **2018**, *8*, 24.

(3) Wang, S.; Ang, H. M.; Tade, M. O. Volatile organic compounds in indoor environment and photocatalytic oxidation: State of the art. *Environ. Int.* **2007**, *33*, 694−705.

(4) Wells, J. R.; Schoemaecker, C.; Carslaw, N.; Waring, M. S.; Ham, J. E.; Nelissen, I.; Wolkoff, P. Reactive indoor air chemistry and health—A workshop summary. *Int. J. Hyg. Environ. Health* **2017**, *220*, 1222−1229.

(5) Hansen, J. S.; Nørgaard, A. W.; Koponen, I. K.; Sørli, J. B.; Paidi, M. D.; Hansen, S. W. K.; Clausen, P. A.; Nielsen, G. D.; Wolkoff, P.; Larsen, S. T. Limonene and its ozone-initiated reaction products attenuate allergic lung inflammation in mice. *J. Immunotoxicol.* **2016**, *13*, 793−803.

(6) Haque, M. M.; Hasan, M.; Islam, M. S.; Ali, M. E. Physico-mechanical properties of chemically treated palm and coir fiber reinforced polypropylene composites. *Bioresour. Technol.* **2009**, *100*, 4903−4906.

(7) Khalil, H. P. S. A.; Shahnaz, S. B. S.; Ratnam, M. M.; Ahmad, F.; Fuaad, N. A. N. Recycle Polypropylene (RPP) - Wood Saw Dust (WSD) Composites - Part 1: The Effect of Different Filler Size and Filler Loading on Mechanical and Water Absorption Properties. *J. Reinf. Plast. Compos.* **2006**, *25*, 1291−1303.

(8) Bledzki, A. K.; Faruk, O. Wood Fibre Reinforced Polypropylene Composites: Effect of Fibre Geometry and Coupling Agent on Physico-Mechanical Properties. *Appl. Compos. Mater.* **2003**, *10*, 365−379.

(9) Beg, M. D. H.; Pickering, K. L. Fiber Pretreatment and Its Effects on Wood Fiber Reinforced Polypropylene Composites. *Mater. Manuf. Processes* **2006**, *21*, 303−307.

(10) Ma, L.; He, L.; Zhang, L. *Effect of Surface Treatments on Tensile Properties of Hemp Fiber Reinforced Polypropylene Composites*, 2017; Vol. *1829*, p 020016.

DOI: 10.1021/acs.langmuir.9b02241
Langmuir XXXX, XXX, XXX−XXX

(11) Karmarkar, A.; Chauhan, S. S.; Modak, J. M.; Chanda, M. Mechanical properties of wood-fiber reinforced polypropylene composites: Effect of a novel compatibilizer with isocyanate functional group. *Composites, Part A* **2007**, *38*, 227−233.
(12) Novák, I.; Pollák, V.; Chodák, I. Study of Surface Properties of Polyolefins Modified by Corona Discharge Plasma. *Plasma Processes Polym.* **2006**, *3*, 355−364.
(13) Sun, C.; Zhang, D.; Wadsworth, L. C. Corona treatment of polyolefin films - A review. *Adv. Polym. Technol.* **1999**, *18*, 171−180.
(14) Gupta, B. S.; Laborie, M.-P. G. Surface Activation and Adhesion Properties of Wood-Fiber Reinforced Thermoplastic Composites. *J. Adhes.* **2007**, *83*, 939−955.
(15) Laborie, M.-P. G.; Gupta, B. Oxyfluorination of Wood-Fiber Reinforced Thermoplastic Composites to Improve Adhesion. *J. Adhes.* **2008**, *84*, 830−846.
(16) Mechanism of Trialkylborane Promoted Adhesion to Low Surface Energy Plastics.pdf.
(17) Sonnenschein, M. F.; Webb, S. P.; Kastl, P. E.; Arriola, D. J.; Harrington, D. R. Mechanism of Trialkylborane Promoted Adhesion to Low Surface Energy Plastics. *Macromolecules* **2004**, *37*, 7974−7978.
(18) Guo, L.-M.; Wang, W. H.; Wang, Q. W.; Yan, N. Decorating wood flour/HDPE composites with wood veneers. *Polymer Composites* **2018**, *39*, 1144.
(19) Hu, W.; Bai, Y.; Zhang, C.; Li, N.; Cheng, B. Coating based on the modified chlorinated polypropylene emulsion for promoting printability of biaxially oriented polypropylene film. *J. Adhes. Sci. Technol.* **2018**, *32*, 50−67.
(20) Tomasetti, E.; Vandorpe, S.; Daoust, D.; Boxus, T.; Marchand-Brynaert, J.; Poleunis, C.; Bertrand, P.; Legras, R.; Rouxhet, P. G. Diffusion of an adhesion promoter (chlorinated polypropylene) into polypropylene/ethylene-propylene copolymer (PP/EP) blends: method of quantification. *J. Adhes. Sci. Technol.* **2000**, *14*, 779−789.
(21) Ozcan, S.; Ozcifci, A.; Hiziroglu, S.; Toker, H. Effects of heat treatment and surface roughness on bonding strength. *Constr. Build. Mater.* **2012**, *33*, 7−13.
(22) Uehara, K.; Sakurai, M. Bonding strength of adhesives and surface roughness of joined parts. *Journal of Materials Processing Tech* **2002**, *127*, 178−181.

DOI: 10.1021/acs.langmuir.9b02241
Langmuir XXXX, XXX, XXX−XXX